

## Study of 1,4-Dihydropyridine Structural Scaffold: Discovery of Novel Sirtuin Activators and Inhibitors

Antonello Mai,<sup>\*,†</sup> Sergio Valente,<sup>†</sup> Sarah Meade,<sup>‡</sup> Vincenzo Carafa,<sup>§</sup> Maria Tardugno,<sup>†</sup> Angela Nebbioso,<sup>§</sup> Andrea Galmozzi,<sup>||</sup> Nico Mitro,<sup>||,⊥</sup> Emma De Fabiani,<sup>||</sup> Lucia Altucci,<sup>§</sup> and Aleksey Kazantsev<sup>‡</sup>

<sup>†</sup>Istituto Pasteur—Fondazione Cenci Bolognetti, Dipartimento di Chimica e Tecnologie del Farmaco, Università degli Studi di Roma “La Sapienza”, P.le A. Moro 5, 00185 Roma, Italy, <sup>‡</sup>Harvard Medical School, Massachusetts General Hospital, CNY114 16th Street, Charlestown, Massachusetts 02129, <sup>§</sup>Dipartimento di Patologia Generale, Seconda Università degli Studi di Napoli, Vico L. De Crecchio 7, 80138 Napoli, Italy, <sup>||</sup>Dipartimento di Scienze Farmacologiche, Università degli Studi di Milano, Via Balzaretti 9, 20133 Milano, Italy, and <sup>⊥</sup>Giovanni Armenise Harvard Foundation Laboratory, Boston, Massachusetts

Received May 27, 2009

NAD<sup>+</sup>-dependent sirtuin deacetylases have emerged as potential therapeutic targets for treatment of human illnesses such as cancer, metabolic, cardiovascular, and neurodegenerative diseases. The benefits of sirtuin modulation by small molecules have been demonstrated for these diseases. In contrast to the discovery of inhibitors of SIRT1, -2, and -3, only activators for SIRT1 are known. Here, we rationalized the potential of the previously unexplored dihydropyridine scaffold in developing sirtuin ligands, thus we prepared a series of 1,4-dihydropyridine-based derivatives **1–3**. Assessment of their SIRT1–3 deacetylase activities revealed the importance of the substituent at the N1 position of the dihydropyridine structure on sirtuin activity. Placement of cyclopropyl, phenyl, or phenylethyl groups at N1 conferred nonselective SIRT1 and SIRT2 inhibition activity, while a benzyl group at N1 conferred potent SIRT1, -2, and -3 activation. Senescence assays performed on hMSC and mitochondrial function studies conducted with murine C2C12 myoblasts confirmed the compounds' novel and unique SIRT-activating properties.

### Introduction

Acetylation/deacetylation of the  $\epsilon$ -amino group of lysine residues in histone tails is a well-known mechanism of regulation of gene expression and transcription.<sup>1</sup> Among the histone deacetylase (HDAC<sup>a</sup>) enzyme families, the class III HDACs, also named sirtuins from their founding member in yeast, silent information regulator 2 (Sir2), share peculiar features that make them very different from the “classical” class I/II/IV HDACs.<sup>2,3</sup> Indeed, the human sirtuins (SIRT1–SIRT7) do not have any sequence similarity with the other HDACs, they act through a NAD<sup>+</sup>-dependent mechanism of catalysis (instead of the Zn<sup>2+</sup>-dependent deacetylation used by HDACs), and are not sensitive to the common HDAC inhibitors.<sup>4–6</sup> In regard to their roles in physiology and pathology, sirtuins are multifaceted enzymes that regulate a variety of cellular functions, from controlling gene expression and genome maintenance to longevity and metabolism.<sup>7–10</sup>

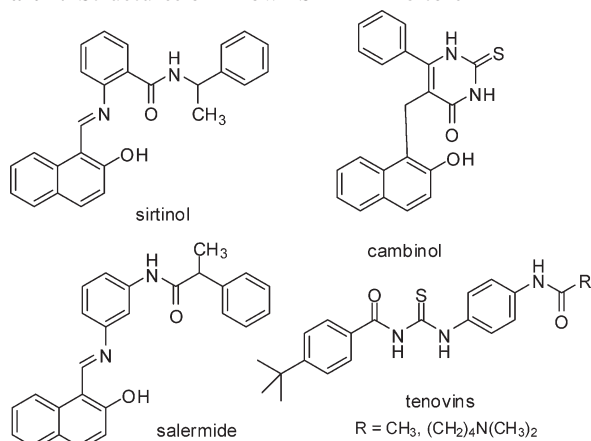
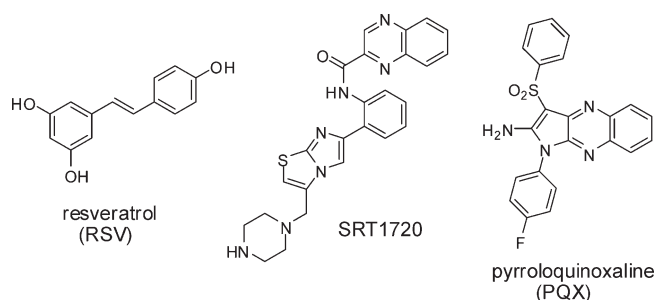
SIRT1, the sirtuin member with the highest sequence similarity (48%) with yeast Sir2, has recently been found to be involved in a variety of diseases such as cancer and metabolic disorders as well as cardiovascular and neurodegenerative diseases, mainly through deacetylation of nonhistone substrates such as the tumor suppressor protein p53, the histone acetyltransferase (HAT) enzyme p300, members of the forkhead box class O (FOXO) family, peroxisome proliferator-activated receptor  $\gamma$  (PPAR $\gamma$ ) coactivator 1 $\alpha$  (PGC-1 $\alpha$ ), and nuclear factor- $\kappa$ B (NF- $\kappa$ B).<sup>11–13</sup>

SIRT1, through its negative regulation of p53 and concomitant positive regulation of the oncogene B-cell lymphoma 6 (BCL6) protein, and through induction of the FOXO-1-dependent vascular endothelial growth factor-C (VEGF-C), may repress apoptosis and enhance tumor growth, angiogenesis, and metastasis.<sup>14–16</sup> In addition, SIRT1 has been found to be upregulated in human lung cancer, prostate cancer, colon carcinoma, and leukemia, highlighting the potential use of SIRT inhibitors (SIRTi) as anticancer agents.<sup>17,18</sup>

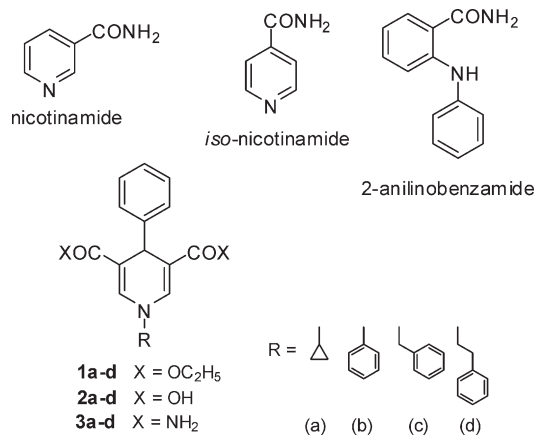
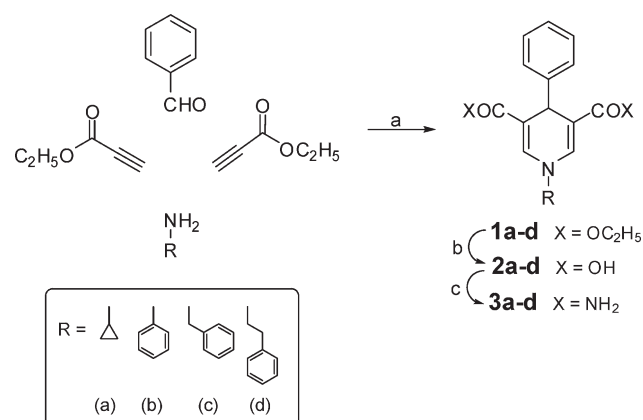
Indeed, inhibitors such as sirtinol have been reported to induce senescence-like growth arrest in human breast cancer MCF-7 cells and lung cancer H1299 cells, cambinol induced apoptosis in BCL6-expressing Burkitt lymphoma cells,<sup>20</sup> and salermide, recently reported by us, was well tolerated by mice at concentrations up to 100  $\mu$ M and prompted tumor-specific, p53-independent apoptosis in a wide range of human cancer cell lines.<sup>21</sup> Furthermore, tenovins<sup>22</sup> were identified via a yeast genetic screen for p53 activators and decreased tumor growth in vivo as single agents at low micromolar concentrations (Chart 1).

\*To whom correspondence should be addressed. Phone: +3906-4991-3392. Fax: +3906-491491. E-mail: antonello.mai@uniroma1.it.

<sup>a</sup>Abbreviations: BCL6, B-cell lymphoma 6; CD11c-PE, phycoerythrin-conjugated CD11c; DHP, 1,4-dihydropyridine; eNOS, endothelial NO synthase; FOXO, forkhead box class O; HAT, histone acetyltransferase; HDAC, histone deacetylase; HDL, high-density lipoprotein; hMSC, human mesenchymal stem cells; HUVEC, human umbilical vein endothelial cells; LXR, liver X receptor; mTFA, mitochondrial transcription factor A; NF- $\kappa$ B, nuclear factor- $\kappa$ B; NRF, nuclear respiratory factor; PBS, phosphate buffered saline; PGC-1 $\alpha$ , peroxisome proliferator-activated receptor  $\gamma$  coactivator 1 $\alpha$ ; PI, propidium iodide; PML, promyelocytic leukemia; PPAR $\gamma$ , peroxisome proliferator-activated receptor  $\gamma$ ; RSV, resveratrol; SAHA, suberoylanilide hydroxamic acid; SA- $\beta$ -gal, senescence-associated  $\beta$ -galactosidase; Sir2, silent information regulator 2; STACs, sirtuin activating compounds; VEGF-C, vascular endothelial growth factor-C;  $\beta$ -gal,  $\beta$ -galactosidase.

**Chart 1.** Structures of Known SIRT Inhibitors**Chart 2.** Structures of Known SIRT Activators

Conversely, SIRT1 may have some beneficial effects in carcinogenesis, through its deacetylation activity on Ku70 and resultant Ku70-associated increase of DNA repair activity.<sup>23</sup> Additionally, deacetylation of  $\beta$ -catenin results in inactivation of transcription and halts cell proliferation.<sup>24</sup> SIRT1 displays a protective role in cardiovascular diseases, likely through its activation of the liver X receptor (LXR) gene, resulting in beneficial effects in HDL synthesis, cholesterol transport, and atherosclerosis.<sup>25</sup> In addition, through eNOS deacetylation, SIRT1 improves endothelial cell survival and functions.<sup>26</sup> A neuroprotective role has been evocated for SIRT1, associated with its downregulation of pro-apoptotic factors and activation of PGC-1 $\alpha$ ,<sup>12,27,28</sup> as PGC-1 $\alpha$  mediates the regulatory role of SIRT1 in metabolic homeostasis, consumption of oxygen in muscle fibers, mitochondrial function, and mitochondrial biogenesis.<sup>29</sup> Last but not least, an increase in Sir2 levels extended lifespan in yeast, *Caenorhabditis elegans*, and *Drosophila*, while a deletion or mutation in Sir2 gave an opposite effect.<sup>2,3,9</sup> In humans, SIRT1 activity can overcome p53/PML-induced senescence<sup>30</sup> and negatively regulates mSIN3A/HDAC1 transcriptional repression activity, inhibiting cell growth arrest and cellular senescence.<sup>31</sup> Resveratrol (RSV, Chart 2), the first reported SIRT1 activator, has been shown to extend lifespan in yeast, *C. elegans*, *Drosophila*, and rodents.<sup>29,32</sup> With respect to the number of SIRTi described in the literature, only a few SIRT activators have been disclosed up to now. Aside from RSV and other polyphenolic compounds (sirtuin activating compounds, STACs),<sup>33</sup> two series of small molecule SIRT activators, imidazo[1,2-*b*]thiazoles (such as SRT1720, Sirtris Pharmaceuticals)<sup>34</sup> and pyrrolo[3,2-*b*]quinoxalines (such as PQX, S\*Bio Pte Ltd.)<sup>35</sup> (Chart 2), have been recently described as oral antidiabetic and lipolytic/anti-inflammatory agents, respectively.

**Figure 1.** Novel 1,4-dihydropyridine (DHP) compounds and related derivatives.**Scheme 1<sup>a</sup>**


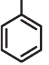
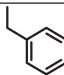
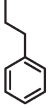

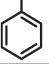
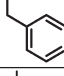
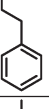

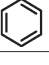
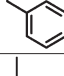

<sup>a</sup> (a) CH<sub>3</sub>COOH, 80 °C. (b) 5 N KOH, EtOH, 80 °C. (c) (1) Et<sub>3</sub>N, Bop reagent, dry DMF, rt, 30 min, N<sub>2</sub> atmosphere; (2) 33% aq NH<sub>3</sub>, dry DMF, rt, 30 min, N<sub>2</sub> atmosphere.

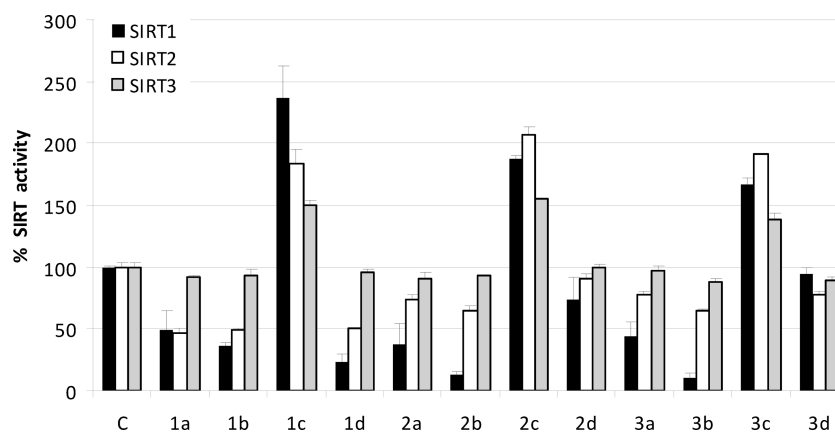
To pursue our researches on sirtuin modulating compounds,<sup>21,36</sup> we started with the information that nicotinamide inhibited SIRT at the micromolar level,<sup>37</sup> whereas isonicotinamide has been reported as a SIRT activator<sup>38</sup> (Figure 1). In addition, Suzuki et al. screened a focused library containing hydroxy-, alkoxy-, and anilino-benzamides, phthalimide, quinazolones, amino- and alkoxy-nicotinamides, and 3-carboxamidopyridinium ions, identifying a series of 2-anilinobenzamides as SIRT1 inhibitors<sup>39</sup> (Figure 1). Thus, we decided to explore the 1,4-dihydropyridine scaffold for the design of new compounds, potentially active as sirtuin modulators. Using a three-component (aliphatic/aromatic amine, ethyl propiolate, and benzaldehyde), one-pot reaction, we prepared some 3,5-dicarbethoxy-, 3,5-dicarboxy-, and 3,5-dicarboxamido-4-phenyl-1,4-dihydropyridines **1a-d**, **2a-d**, and **3a-d**, respectively, and we tested them against human SIRT1, SIRT2, and SIRT3.

## Chemistry

The 3,5-dicarbethoxy-4-phenyl-1,4-dihydropyridines **1a-d** were prepared by cyclocondensation between benzaldehyde, ethyl propiolate and the opportune amine, heated at 80 °C in glacial acetic acid. Furthermore, compounds **1a-d** underwent alkaline hydrolysis at 80 °C in ethanol to furnish the

**Table 1.** Chemical and Physical Data of Compounds 1–3

compd	lab code	R	X	mp, °C	recrystallization solvent	yield, %
<b>1a</b>	MC2733		OEt	100-102	cyclohexane	75
<b>1b</b> <sup>40</sup>	MC2734		OEt	143-145	cyclohexane/benzene	60
<b>1c</b> <sup>41</sup>	MC2562		OEt	139-141	cyclohexane/benzene	78
<b>1d</b>	MC2735		OEt	91-93	cyclohexane	68
<b>2a</b>	MC2736		OH	220-222	methanol	87
<b>2b</b> <sup>40</sup>	MC2737		OH	240-242	methanol	83
<b>2c</b> <sup>42</sup>	MC2563		OH	191-193	acetonitrile/methanol	86
<b>2d</b>	MC2738		OH	218-220	acetonitrile/methanol	85
<b>3a</b>	MC2743		NH <sub>2</sub>	>250	methanol	72
<b>3b</b>	MC2744		NH <sub>2</sub>	194-196	acetonitrile/methanol	69
<b>3c</b>	MC2566		NH <sub>2</sub>	>250	methanol	74
<b>3d</b>	MC2745		NH <sub>2</sub>	>250	methanol	70

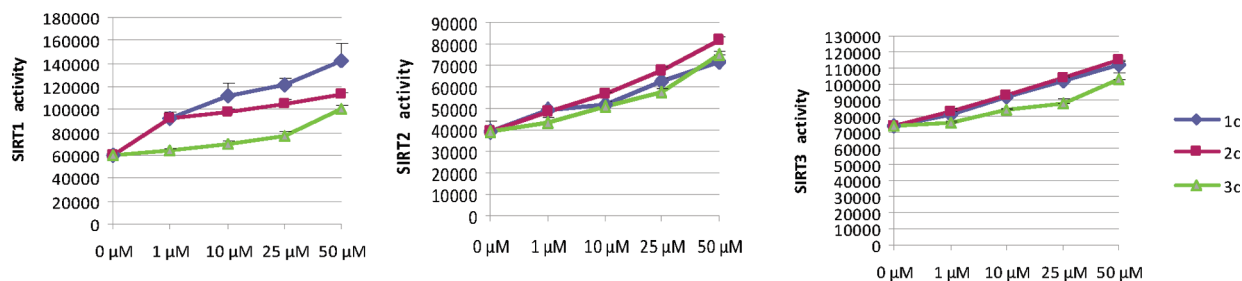
**Figure 2.** SIRT1, -2, and -3 modulating activities of compounds 1–3 tested at 50 μM.

corresponding 3,5-dicarboxy derivatives **2a–d**. Finally, these last compounds reacted with triethylamine, benzotriazole-1-yloxytris(dimethylamino)phosphonium hexafluorophosphate (Bop reagent), and 33% aqueous ammonia under N<sub>2</sub> atmosphere to give the 3,5-diamides **3a–d** (Scheme 1). Among the synthesized derivatives, compounds **1b**, **1c**, and their corresponding acids **2b** and **2c** are known in the literature

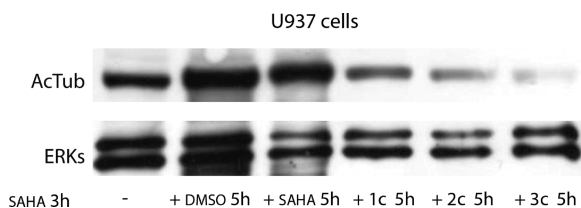
(**1b** and **2b**,<sup>40</sup> **1c**,<sup>41</sup> **2c**<sup>42</sup>). Chemical and physical data for compounds 1–3 are reported in Table 1.

## Results and Discussion

**SIRT1, -2, and -3 Modulator Activity: Enzyme and Functional Assays.** All the prepared compounds were tested against human SIRT1, SIRT2, and SIRT3 at 50 μM, using the Fluor



**Figure 3.** Dose-dependent SIRT1, -2, and -3 activation by the *N*-benzyl DHPs **1c**, **2c**, and **3c**.



**Figure 4.** Effects of SIRT activators **1c**, **2c**, and **3c** ( $50 \mu\text{M}$ ) on  $\alpha$ -tubulin acetylation in SAHA-pretreated U937 cells.

de Lys fluorescent biochemical assay (BioMol) (Figure 2. Absolute values of SIRT modulation activities by **1–3** have been reported as Supporting Information, Figure S1). The new 1,4-dihydropyridine (DHP) derivatives **1–3** showed a wide range of SIRT modulating activities, depending on their substituent at the N1 position and/or at the 3,5 position of the DHP ring. In particular, compounds carrying a cyclopropyl, a phenyl, or a phenylethyl group at N1 inhibited SIRT1 and, to a lesser extent, SIRT2, while they were inactive against SIRT3. The highest SIRT1 inhibition activities were seen with the N1-phenyl analogues bearing a carboxy or a carboxamido group at the 3,5 positions (**2b** and **3b**, 86.6% and 89.1% of SIRT1 inhibition at  $50 \mu\text{M}$ ), followed by the 1-phenethyl- and 1-phenyl-3,5-dicarboxy derivatives **1d** and **1b** (76.6% and 63.6% of inhibition, respectively). Against SIRT2, the diester compounds **1a**, **1b**, and **1d** showed the highest inhibition activity, with comparable potency (**1a**: 53.7%; **1b**: 51.3%; **1d**: 49.6% of SIRT2 inhibiting activity at  $50 \mu\text{M}$ ).

Surprisingly, the DHPs bearing a benzyl group at the N1 position, regardless of their substitution at the 3,5 positions (either a carbethoxy (**1c**), carboxy (**2c**), or carboxamido (**3c**) moiety), did not inhibit the tested sirtuins but behaved as potent, dose-dependent SIRT1, -2, and -3 activators (Figure 3). In the SIRT1 assay, **1c** and **2c** were the most potent derivatives, with a  $\text{EC}_{150}$  (effective concentration able to increase the enzyme activity of 150%) around  $1 \mu\text{M}$ , while the 3,5-dicarboxamide **3c** was less effective ( $\text{EC}_{150} = 36 \mu\text{M}$ ). Against SIRT2, the dicarboxy derivative **2c** displayed the highest activating potency ( $\text{EC}_{150} = 15 \mu\text{M}$ ), followed by the dicarboxy compound **1c** ( $\text{EC}_{150} = 25 \mu\text{M}$ ), while **3c** was less efficient. Also in the SIRT3 assay, although being less effective than in SIRT1 and -2 assays, **1c** and **2c** exhibited higher activation activity than **3c** ( $\text{EC}_{150}$  values: **1c** and **2c**, around  $50 \mu\text{M}$ ; **3c**,  $> 50 \mu\text{M}$ ).

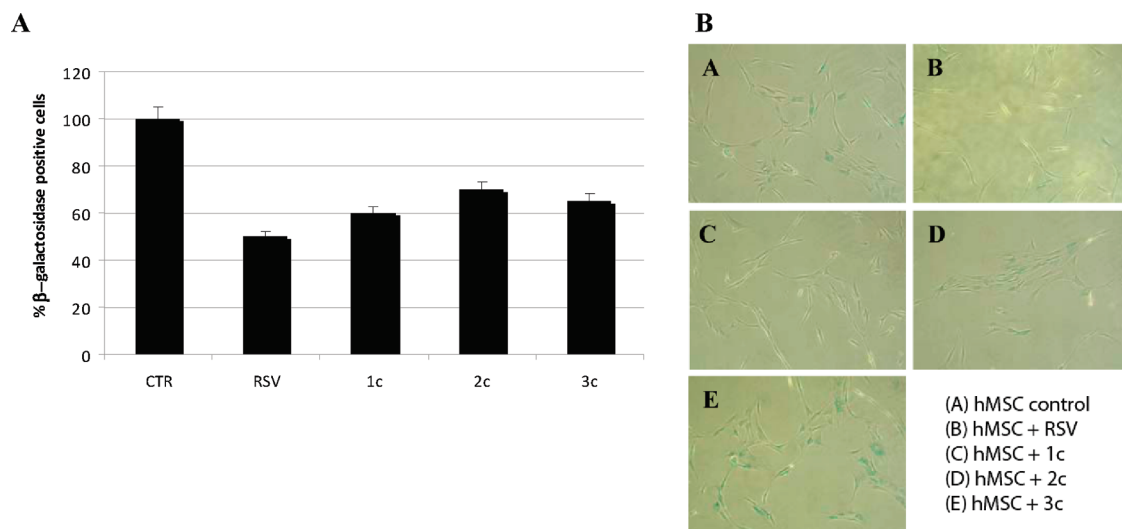
The new SIRT activators **1c**, **2c**, and **3c** were tested in functional assay to determine their effect on acetylation level of  $\alpha$ -tubulin, a known substrate for SIRT2. Western blot analysis was performed on the human leukemia U937 cell line. Because U937 cells typically show weak basal acetylation levels for  $\alpha$ -tubulin,<sup>43,44</sup> the expected hypoacetylation effect from the SIRT activators may be difficult to appreciate. Thus, we pretreated the cells with the well-known

HDAC inhibitor SAHA<sup>45</sup> (suberoylanilide hydroxamic acid, 3 h,  $5 \mu\text{M}$ ) to amplify the acetylation of  $\alpha$ -tubulin.<sup>43,44</sup> After the wash out at 3 h of SAHA incubation, the effects of **1c**, **2c**, and **3c**, used at  $50 \mu\text{M}$ , in comparison with vehicle or SAHA treatment ( $5 \mu\text{M}$ ) on tubulin acetylation levels after 5 h of treatment, have been assessed. As depicted in Figure 4, the tested *N*-benzyl-DHP compounds induced hypoacetylation on  $\alpha$ -tubulin in U937 cells. In SAHA-untreated U937 cells, the SIRT activators showed no effects on tubulin acetylation (data not shown).

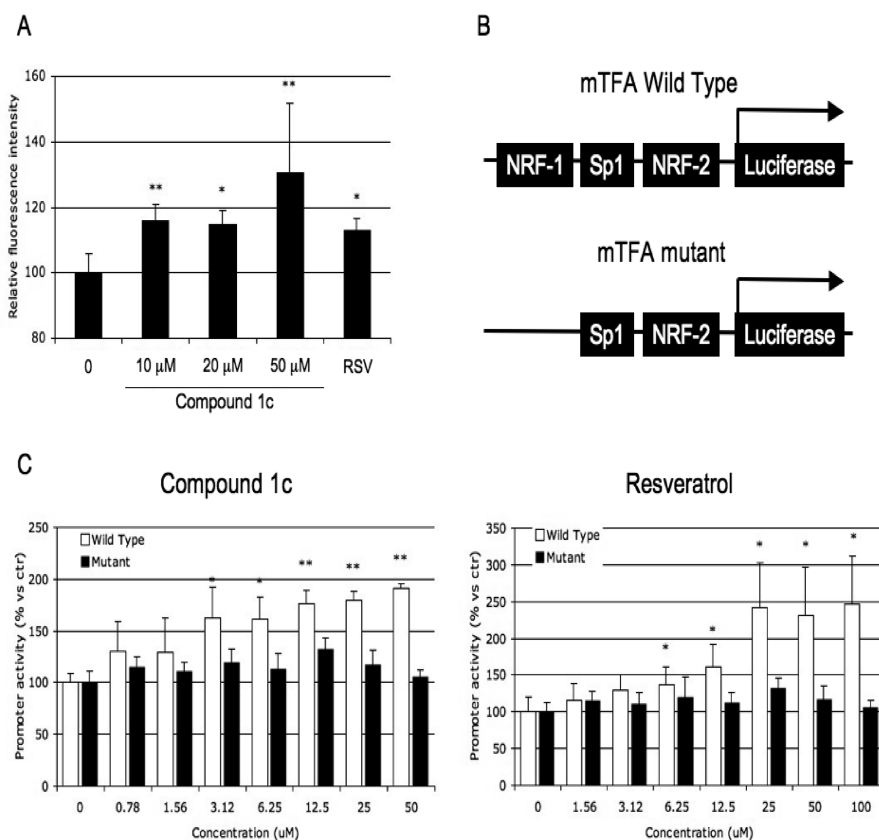
**Biological Cellular Activities.** All the epigenetic modulators prepared in our lab are routinely tested, initially, in the human U937 leukemia cell line, to study their effects on cell cycle, apoptosis induction, and granulocytic differentiation.<sup>46</sup> As such, compounds **1–3** were tested in U937 cells at  $50 \mu\text{M}$  for 30 h and displayed marginal effects in these experimental conditions (Supporting Information, Figure S2). In particular, the three SIRT activators **1c**, **2c**, and **3c** arrested the cell cycle at the G1/S phase, with an effect that could be related to p53 deacetylation as well as to effects on multiple targets within the cell, while a slight if at all apoptotic induction (3–4%) was observed with the diester inhibitors **1a**, **1b**, and **1d**. Granulocytic differentiation was evaluated by the increase of expression of CD11c positive, propidium iodide (PI) negative cells: in this assay, only the diethyl 1-phenethyl-4-phenyl-1,4-dihydropyridine-3,5-dicarboxylate **1d** gave a significant (12.3%) increase, with an effect that seems not to be related to its SIRT1 and -2 inhibition activity. When tested in the MCF-7 breast cancer cell lines, these compounds did not show significant effects, thus suggesting to exert marginal antitumor activities both in hematological and solid cancer models (data not shown).

Inhibition of SIRT1 by sirtinol or splitomicin (another well-known SIRT1 identified through a phenotypic screening in yeast) induced senescence in the H1299,<sup>19</sup> HUVEC,<sup>47</sup> and MCF-7<sup>19</sup> cell lines. In addition, SIRT1 has been reported to gradually decrease in aging cells,<sup>48</sup> whereas SIRT1 activity was able to overcome p53/PML-induced senescence.<sup>30</sup> Thus, agents able to improve SIRT1 activity could be useful against senescence, and indeed RSV has been shown to increase lifespan in many species including rodents.<sup>32</sup> Normal primary cells proliferate in culture for a limited number of doublings prior to undergoing an irreversible growth-arrested stage called replicative senescence, acquiring a senescent phenotype. The most used biomarker for senescent and aging cells is senescence-associated  $\beta$ -galactosidase (SA- $\beta$ -gal), which identifies the senescent cells after cytoplasmatic coloration in blue color.<sup>49</sup> From these data, we tested our SIRT activators **1c**, **2c**, and **3c** (all used at  $50 \mu\text{M}$ ) in primary human mesenchymal stem cells (hMSC), to determine their potential protection against senescence. RSV ( $50 \mu\text{M}$ ) has





**Figure 5.**  $\beta$ -Galactosidase assay in hMSC. (A) Percent of  $\beta$ -gal positive hMSC treated with RSV, **1c**, **2c**, or **3c** at  $50 \mu\text{M}$  for 48 h. (B) Optic microscope images ( $10\times$ ) of treated hMSC.



**Figure 6.** Mitochondrial function in C2C12 myoblasts. (A) Fluorescence intensity of C2C12 myoblasts treated for 16 h with DMSO (0), or increasing concentrations of **1c**, or  $50 \mu\text{M}$  RSV, and stained with Mitotracker Green. The data represent the values obtained after subtraction of the mean fluorescence background (unstained cells). (B) Scheme of the constructs carrying the wild type and mutant mTFA promoters. (C) Transcriptional activity of wild type (white bars) and mutant (black bars) mTFA promoter in C2C12 myoblasts treated for 16 h with increasing concentrations of **1c** (left panel) and RSV (right panel). \*  $p < 0.05$ , \*\*  $p < 0.01$  versus DMSO (0) treated cells (Student's  $t$ -test).

been used as a reference drug. After 48 h of treatment, the number of  $\beta$ -galactosidase positive cells, used as a marker of senescence, have been counted (Figure 5A). Optic microscopy images ( $10\times$ ) of the cell cultures have been also obtained (Figure 5B). In these conditions, considering the amount of senescent positive cells in the control population as 100%, **1c**, **2c**, and **3c** gave 60%, 70%, and 65% positive

cells, respectively, in comparison with 50% positive cells by RSV.

Because RSV was reported to improve mitochondrial function in skeletal muscle, largely due to PGC-1 $\alpha$  activation,<sup>29</sup> we tested the ability of our SIRT activator **1c** to modulate mitochondrial function in murine C2C12 myoblasts. As shown in Figure 6A, treatment with compound **1c**

for 16 h led to a significant increase of fluorescence intensity due to the mitochondrial specific probe Mitotracker Green, indicating increased mitochondrial density. The effect was similar to that observed with 50  $\mu$ M RSV. Mitochondrial transcription factor A (mTFA) is crucial for mitochondrial DNA replication/transcription, and it was described that its expression is controlled by transcription factors belonging to the nuclear respiratory factor (NRF) family and by PGC-1 $\alpha$ .<sup>50</sup> Therefore, we investigated whether SIRT activators were able to increase the transcriptional activity of the mTFA promoter bearing the binding site for NRF1 (Figure 6B), whose activity is PGC-1 $\alpha$ -dependent. We found that both compound **1c** (Figure 6C, left panel) and RSV (Figure 6C, right panel) stimulated the promoter activity in a dose-dependent manner. The effect of both the SIRT activators is PGC-1 $\alpha$ -dependent as the effect was not seen upon deletion of the NRF1 site.

## Conclusion

In conclusion, we have reported the first investigation of DHP-based compounds on the sirtuin modulation activity. The insertion of either a cyclopropyl, phenyl, or phenethyl group at the N1 position of the DHP ring led to SIRT1 and, to a lesser extent, SIRT2 inhibition. Conversely, the insertion of a benzyl group at the same position furnished three new potent SIRT1, -2, and -3 activators, compounds **1c**, **2c**, and **3c**, lacking the polyphenolic structure of RSV, a pleiotropic drug reported as the first SIRT1 activator. Similarly to RSV, in a senescence assay performed with hMSC, **1c**, **2c**, and **3c** were able to reduce the number of senescent cells up to 40%. Furthermore, when tested in murine C2C12 myoblasts, **1c** showed a dose-dependent increase of mitochondrial function, with a mechanism involving PGC-1 $\alpha$ . Further studies are ongoing to improve the SIRT activation activity of our *N*-benzyl-DHPs and to optimize the inhibition profile of the *N*-cyclopropyl and *N*-phenyl DHPs.

## Experimental Section

**Chemistry.** Melting points were determined on a Buchi 530 melting point apparatus and are uncorrected. Infrared (IR) spectra (KBr) were recorded on a Perkin-Elmer Spectrum One instrument. <sup>1</sup>H NMR and <sup>13</sup>C NMR spectra were recorded at 400 MHz on a Bruker AC 400 spectrometer; chemical shifts are reported in  $\delta$  (ppm) units relative to the internal reference tetramethylsilane (Me<sub>4</sub>Si). All compounds were routinely checked by TLC and <sup>1</sup>H NMR. TLC was performed on aluminum-backed silica gel plates (Merck DC, Alufolien Kieselgel 60 F<sub>254</sub>) with spots visualized by UV light. All solvents were reagent grade and, when necessary, were purified and dried by standard methods. Concentration of solutions after reactions and extractions involved the use of a rotary evaporator operating at reduced pressure of ca. 20 Torr. Organic solutions were dried over anhydrous sodium sulfate. Analytical results are within  $\pm 0.40\%$  of the theoretical values. All chemicals were purchased from Aldrich Chimica, Milan (Italy), or from Lancaster Synthesis GmbH, Milan (Italy), and were of the highest purity.

**General Procedure for the Synthesis of Diethyl 1-Aryl-(or Arylalkyl, or Cycloalkyl)-4-phenyl-1,4-dihydropyridine-3,5-dicarboxylates (1a–d).** Example: Diethyl 1-cyclopropyl-4-phenyl-1,4-dihydropyridine-3,5-dicarboxylate (**1a**). Ethyl propionate (18.84 mmol, 1.9 mL), benzaldehyde (9.42 mmol, 0.96 mL), and cyclopropylamine (9.42 mmol, 0.65 mL) in glacial acetic acid (0.5 mL) were heated at 80 °C for 30 min. After cooling, the mixture was poured into water (20 mL) and stirred for 1 h. The

solid product was filtered and washed with Et<sub>2</sub>O (3  $\times$  30 mL) to give pure **1a**, which was recrystallized by cyclohexane. <sup>1</sup>H NMR (400 MHz, CDCl<sub>3</sub>)  $\delta$  0.83–0.90 (m, 4 H, cyclopropane protons), 1.14–1.17 (t, 6 H, COOCH<sub>2</sub>CH<sub>3</sub>), 2.94–2.99 (m, 1 H, cyclopropane proton), 3.97–4.11 (q, 4 H, COOCH<sub>2</sub>CH<sub>3</sub>), 4.83 (s, 1 H, PhCH), 7.08–7.23 (m, 5 H, benzene protons), 7.31 (s, 2 H, dihydropyridine protons) ppm. <sup>13</sup>C NMR (400 MHz, CDCl<sub>3</sub>)  $\delta$  6.10 (2C), 14.20 (2C), 38.50, 44.50, 61.70 (2C), 108.0 (2C), 125.80, 128.70 (2C), 129.10 (2C), 142.20, 146.10 (2C), 167.20 (2C) ppm. MS (EI): *m/z*: 341 (*M*)<sup>+</sup>.

**General Procedure for the Synthesis of 1-Aryl-(or Arylalkyl, or Cycloalkyl)-4-phenyl-1,4-dihydropyridine-3,5-dicarboxylic Acids (2a–d).** Example: 1-Phenethyl-4-phenyl-1,4-dihydropyridine-3,5-dicarboxylic acid (**2d**). A mixture of **1d** (1.23 mmol, 0.5 g) and 5 N KOH (6.15 mmol, 0.34 g, 1.23 mL) in ethanol (10 mL) was stirred at 80 °C overnight. Afterward, the solvent was evaporated, the residue was eluted with water (30 mL), and the resulting solution acidified with 2 N HCl. The obtained precipitate was filtered, washed with water (3  $\times$  30 mL) and dried to afford pure compound **2d**, which was recrystallized by acetonitrile/methanol. <sup>1</sup>H NMR (400 MHz, DMSO-*d*<sub>6</sub>)  $\delta$  2.95–2.99 (t, 2 H, PhCH<sub>2</sub>CH<sub>2</sub>), 3.61–3.65 (t, 2 H, PhCH<sub>2</sub>CH<sub>2</sub>), 4.82 (s, 1 H, PhCH), 7.07–7.34 (m, 12 H, benzene protons and dihydropyridine protons), 12.00 (bs, 2 H, COOH) ppm. <sup>13</sup>C NMR (400 MHz, DMSO-*d*<sub>6</sub>)  $\delta$  42.00, 43.80, 57.70, 107.30 (2C), 125.70, 125.90, 127.70 (4C), 128.60 (4C), 139.40, 144.40, 148.90 (2C), 171.30 (2C) ppm. MS (EI): *m/z*: 349 (*M*)<sup>+</sup>.

**General Procedure for the Synthesis of 1-Aryl-(or Arylalkyl, or Cycloalkyl)-4-phenyl-1,4-dihydropyridine-3,5-dicarboxamides (3a–d).** Example: 1-Phenyl-4-phenyl-1,4-dihydropyridine-3,5-dicarboxamide (**3b**). Triethylamine (10.38 mmol, 1.44 mL) and BOP reagent (3.12 mmol, 1.38 g) were added under nitrogen atmosphere to a solution of compound **2b** (0.47 mmol, 0.150 g) in dry DMF (5 mL), and the resulting mixture was stirred for 30 min at room temperature. Afterward, 33% aqueous ammonia (4.7 mmol, 0.27 mL) was added, and the resulting mixture was stirred for further 30 min. The reaction was quenched with water (30 mL), the filtered precipitate was washed with water (3  $\times$  30 mL) and Et<sub>2</sub>O (3  $\times$  30 mL) to provide **3b**, which was recrystallized by acetonitrile/methanol. <sup>1</sup>H NMR (DMSO-*d*<sub>6</sub>)  $\delta$  5.07 (s, 1 H, PhCH), 6.73 (bs, 4 H, CONH<sub>2</sub>), 7.02–7.53 (m, 12 H, benzene protons and dihydropyridine protons) ppm. <sup>13</sup>C NMR (400 MHz, DMSO-*d*<sub>6</sub>)  $\delta$  45.10, 110.20 (2C), 116.30 (2C), 118.80, 125.80, 128.70 (2C), 129.60 (2C), 138.10 (2C), 141.30, 142.20, 171.0 (2C) ppm. MS (EI): *m/z*: 319 (*M*)<sup>+</sup>.

**SIRT Assay.** Modulation of sirtuin activity by compounds was assessed using the Fluor de Lys fluorescent biochemical assay available through BioMol International, LP in 96-well format. In the first part of a two-step reaction, an acetylated lysine side chain present on the substrate is deacetylated during incubation at 37 °C for an hour with active enzyme (SIRT1, SIRT2, or SIRT3), compounds **1–3**, and NAD<sup>+</sup> in white, 96-well polystyrene luminescence plates (Perkin-Elmer-6005680). The latter half of the reaction produces a fluorophore upon treatment with a developing reagent. The reaction is read by a Perkin-Elmer Victor<sup>2</sup>V 1420 Multilabel Counter plate reader with filters that excite at 355 nm and detect emitted light at 460 nm with a read time of 0.1s per well.

Sirtuin 1 enzyme (BioMol-SE-239) is a 747 amino acid protein with a molecular weight of 82 kDa, while Sirtuin 2 enzyme (BioMol-SE-251) is a 389 amino acid protein with a molecular weight of 43 kDa; both were purified from human cDNA expressed in *Escherichia coli* and stored in 25 mM Tris, pH 7.5, 100 mM NaCl, 5 mM DTT, and 10% glycerol. Sirtuin 3 enzyme (BioMol-SE-270) is inactive prior to removal of its N-terminus, thus this assay only utilizes the catalytically active fragment spanning amino acids 102–299 with a molecular weight of 32.7 kDa. Like sirtuins 1 and 2, the fragment was purified from cDNA expressed in *E. coli* and stored in 25 mM Tris, pH 7.5, 100 mM NaCl, 5 mM DTT, and 10% glycerol.

While there is variability in activity among individual lots, each experiment normalizes SIRT1 activity to 1U/reaction well and SIRT2 and SIRT3 activity to 5U/reaction well (where  $U = 1$  pmol/min at 37 °C, 250  $\mu$ M substrate, and 500  $\mu$ M NAD<sup>+</sup>). All reagents are diluted on ice in the following reaction buffer: 50 mM Tris/Cl, pH 8.0, 137 mM NaCl, 2.7 mM KCl, 1 mM MgCl<sub>2</sub>, and 1 mg/mL BSA. Thus for each reaction well, the requisite amount of enzyme (as detailed above) is added to 500  $\mu$ M NAD<sup>+</sup> (BioMol-KI-282), 250  $\mu$ M fluorogenic deacetylase substrate (BioMol-KI-177), and the compound of interest at a given concentration in a total reaction volume of 50  $\mu$ L. After an hour incubation at 37 °C, the reaction is stopped upon addition of 1 $\times$  Developer (BioMol-KI-176) for a final reaction volume of 100  $\mu$ L. The reaction is incubated at 37 °C for an additional 15 min and then read on the plate reader. Experimental replicates were done in triplicate with appropriate controls. Positive controls contained only enzyme, substrate, NAD<sup>+</sup>, and DMSO while background controls contained substrate, NAD<sup>+</sup>, and DMSO only. Autofluorescent controls were also included for testing of activators and included substrate, NAD<sup>+</sup>, and the compound at the same concentration as its experimental counterpart. Background signal was subtracted from positive control well signals, and autofluorescent background was subtracted from experimental well signals at all tested compound doses.

**Determination of  $\alpha$ -Tubulin Specific Acetylation.** For  $\alpha$ -tubulin acetylation studies, 50  $\mu$ g of total protein extracts (U937 cells) were separated on a 10% polyacrylamide gels and blotted.<sup>51</sup> Western blots were shown for acetylated  $\alpha$ -tubulin (Sigma, dilution 1:500) and total ERKs (Santa Cruz) were used to normalize for equal loading.

**Cell Cycle Analysis on U937 Cells.** First,  $2.5 \times 10^5$  cells were collected and resuspended in 500  $\mu$ L of a hypotonic buffer (0.1% Triton X-100, 0.1% sodium citrate, 50  $\mu$ g/mL propidium iodide (PI), RNase A). Then cells were incubated in the dark for 30 min. Samples were acquired on a FACS-Calibur flow cytometer using the Cell Quest software (Becton Dickinson) and analyzed with standard procedures using the Cell Quest software (Becton Dickinson) and the ModFit LT version 3 Software (Verity) as previously reported.<sup>51</sup> All experiments were completed in triplicate.

**FACS Analysis of Apoptosis on U937 Cells.** Apoptosis was measured with the caspase 3–7 detection (B-Bridge) method; samples were analyzed by FACS with Cell Quest technology (Becton Dickinson) as previously reported.<sup>52</sup>

**Granulocytic Differentiation on U937 Cells.** Granulocytic differentiation was carried out as previously described.<sup>52</sup> U937 cells were harvested and resuspended in 10  $\mu$ L phycoerythrin-conjugated CD11c (CD11c-PE). Control samples were incubated with 10  $\mu$ L of PE conjugated mouse IgG1, incubated for 30 min at 4 °C in the dark, washed in PBS, and resuspended in 500  $\mu$ L of PBS containing PI (0.25  $\mu$ g/mL). Samples were analyzed by FACS with Cell Quest technology (Becton Dickinson). PI positive cells have been excluded from the analysis.

**$\beta$ -Galactosidase Assay.** For this assay, we used  $3 \times 10^5$  cells/well. Human primary mesenchymal stem cells have been kept in culture for 30 days (corresponding to the ninth passage) before starting the experiment. Cultured cells were washed in PBS and fixed with 2% (w/v) formaldehyde and 0.2% (w/v) glutaraldehyde solution. Cells were then washed with PBS and incubated overnight at 37 °C in freshly prepared staining buffer (30 mM citric acid/ phosphate buffer (pH 6), 5 mM K<sub>4</sub>Fe(CN)<sub>6</sub>, 5 mM K<sub>3</sub>Fe(CN)<sub>6</sub>, 150 mM NaCl, 2 mM MgCl<sub>2</sub>, 1 mg/mL X-Gal). At the end of incubation, cells were washed with PBS and examined under the microscope. The percent of senescent cells was calculated by counting the number of blue cells (positive cells) out of total cells.<sup>49,53</sup>

**Mitochondrial Density in Murine C2C12 Myoblasts.** Murine C2C12 myoblasts were plated in 96-well clusters (3000 cells/

well) and treated overnight with the compounds under investigation. Mitochondria were stained with the Mito-Tracker Green FM dye (200 nM) from Molecular Probes (Invitrogen, Milan, Italy). Fluorescence intensities were measured using the EnVision multilabel reader platform (PerkinElmer, Italia Spa, Monza, Italy). The data shown represent the values obtained after subtraction of the mean fluorescence background measured in wells with unstained cells.

**Transcriptional Activity of mTFA-Promoter in Murine C2C12 Myoblasts.** Murine C2C12 myoblasts (CRL-1772, ATCC, Teddington, UK) were grown in Dulbecco's Modified Eagle's Medium supplemented with 10% heat inactivated fetal calf serum. Cells were retrotransfected with the plasmids bearing either the mTFA-promoter or the mutated form lacking the NRF1 binding site,<sup>50</sup> fused to the luciferase gene. Lipofectamine (Invitrogen, Milan, Italy) was used as transfecting reagent (2.5  $\mu$ L/ $\mu$ g DNA). Transfected cells were then plated in 96-well clusters (3000 cells/well) and treated overnight with the compounds under investigation. The luciferase activity was measured using the EnVision multilabel reader platform (PerkinElmer Italia Spa, Monza, Italy). The constructs used in the transfection assays were first validated overexpressing PGC-1 $\alpha$  or SIRT1. In both conditions the wild type promoter was stimulated by 2–3 fold, whereas the mutant promoter lacking the NRF1 binding site did not respond.

**Acknowledgment.** This work was supported by grants from AIRC, RETI FIRB, European Union (APOSYS, ATLAS), Fondazione Luigi Califano ONLUS, Fondazione Roma, and RJG and Carmen's Foundations.

**Supporting Information Available:** Elemental analyses and <sup>1</sup>H NMR/<sup>13</sup>C NMR/mass spectra of compounds 1–3. Absolute values of modulation of SIRT1, -2, and -3 activities by 1–3. Effects of 1–3 (50  $\mu$ M, 30 h) on cell cycle, apoptosis induction, and granulocytic differentiation in human U937 leukemia cells. This material is available free of charge via the Internet at <http://pubs.acs.org>.

## References

- (1) Grunstein, M. Histone acetylation in chromatin structure and transcription. *Nature* **1997**, *389*, 349–352.
- (2) Michan, S.; Sinclair, D. Sirtuins in mammals: insights into their biological function. *Biochem. J.* **2007**, *404*, 1–13.
- (3) Haigis, M. C.; Guarente, L. P. Mammalian sirtuins—emerging roles in physiology, aging, and calorie restriction. *Genes Dev.* **2006**, *20*, 2913–21.
- (4) Imai, S.; Armstrong, C. M.; Kaerberlein, M.; Guarente, L. Transcriptional silencing and longevity protein Sir2 is an NAD-dependent histone deacetylase. *Nature* **2000**, *403*, 795–800.
- (5) Jackson, M. D.; Denu, J. M. Structural identification of 2'- and 3'-O-acetyl-ADP-ribose as novel metabolites derived from the Sir2 family of beta-NAD<sup>+</sup>-dependent histone/protein deacetylases. *J. Biol. Chem.* **2002**, *277*, 18535–18544.
- (6) Borra, M. T.; O'Neill, F. J.; Jackson, M. D.; Marshall, B.; Verdin, E.; Foltz, K. R.; Denu, J. M. Conserved enzymatic production and biological effect of O-acetyl-ADP-ribose by silent information regulator 2-like NAD<sup>+</sup>-dependent deacetylases. *J. Biol. Chem.* **2002**, *277*, 12632–12641.
- (7) Jiang, W. J. Sirtuins: novel targets for metabolic disease in drug development. *Biochem. Biophys. Res. Commun.* **2008**, *373*, 341–344.
- (8) Taylor, D. M.; Maxwell, M. M.; Luthi-Carter, R.; Kazantsev, A. G. Biological and potential therapeutic roles of sirtuin deacetylases. *Cell. Mol. Life Sci.* **2008**, *65*, 4000–4018.
- (9) Pallas, M.; Verdager, E.; Tajés, M.; Gutierrez-Cuesta, J.; Camins, A. Modulation of sirtuins: new targets for antiaging. *Recent Pat CNS Drug Discovery* **2008**, *3*, 61–69.
- (10) Milne, J. C.; Denu, J. M. The Sirtuin family: therapeutic targets to treat diseases of aging. *Curr. Opin. Chem. Biol.* **2008**, *12*, 11–17.
- (11) Pillarisetti, S. A review of Sirt1 and Sirt1 modulators in cardiovascular and metabolic diseases. *Recent Pat. Cardiovasc. Drug Discovery* **2008**, *3*, 156–64.



- (12) Outeiro, T. F.; Marques, O.; Kazantsev, A. Therapeutic role of sirtuins in neurodegenerative disease. *Biochim. Biophys. Acta* **2008**, *1782*, 363–9.
- (13) Zeng, L.; Chen, R.; Liang, F.; Tsuchiya, H.; Murai, H.; Nakahashi, T.; Iwai, K.; Takahashi, T.; Kanda, T.; Morimoto, S. Silent information regulator, Sirtuin 1, and age-related diseases. *Geriatr. Gerontol. Int.* **2009**, *9*, 7–15.
- (14) Luo, J.; Nikolaev, A. Y.; Imai, S.; Chen, D.; Su, F.; Shiloh, A.; Guarente, L.; Gu, W. Negative control of p53 by Sir2alpha promotes cell survival under stress. *Cell* **2001**, *107*, 137–148.
- (15) Bereshchenko, O. R.; Gu, W.; Dalla-Favera, R. Acetylation inactivates the transcriptional repressor BCL6. *Nat. Genet.* **2002**, *32*, 606–613.
- (16) Li, J.; Wang, E.; Rinaldo, F.; Datta, K. Upregulation of VEGF-C by androgen depletion: the involvement of IGF-IR-FOXO pathway. *Oncogene* **2005**, *24*, 5510–5520.
- (17) Bradbury, C. A.; Khanim, F. L.; Hayden, R.; Bunce, C. M.; White, D. A.; Drayson, M. T.; Craddock, C.; Turner, B. M. Histone deacetylases in acute myeloid leukaemia show a distinctive pattern of expression that changes selectively in response to deacetylase inhibitors. *Leukemia* **2005**, *19*, 1751–1759.
- (18) Yeung, F.; Hoberg, J. E.; Ramsey, C. S.; Keller, M. D.; Jones, D. R.; Frye, R. A.; Mayo, M. W. Modulation of NF-kappaB-dependent transcription and cell survival by the SIRT1 deacetylase. *EMBO J.* **2004**, *23*, 2369–2380.
- (19) Ota, H.; Tokunaga, E.; Chang, K.; Hikasa, M.; Iijima, K.; Eto, M.; Kozaki, K.; Akishita, M.; Ouchi, Y.; Kaneki, M. Sirt1 inhibitor, Sirtinol, induces senescence-like growth arrest with attenuated Ras-MAPK signaling in human cancer cells. *Oncogene* **2006**, *25*, 176–185.
- (20) Heltweg, B.; Gatbonton, T.; Schuler, A. D.; Posakony, J.; Li, H.; Goehle, S.; Kollipara, R.; Depinho, R. A.; Gu, Y.; Simon, J. A.; Bedalov, A. Antitumor activity of a small-molecule inhibitor of human silent information regulator 2 enzymes. *Cancer Res.* **2006**, *66*, 4368–4377.
- (21) Lara, E.; Mai, A.; Calvanese, V.; Altucci, L.; Lopez-Nieva, P.; Martinez-Chantar, M. L.; Varela-Rey, M.; Rotili, D.; Nebbioso, A.; Roperio, S.; Montoya, G.; Oyarzabal, J.; Velasco, S.; Serrano, M.; Witt, M.; Villar-Garea, A.; Inhof, A.; Mato, J. M.; Esteller, M.; Fraga, M. F. Sirtuin inhibitor with a strong cancer-specific proapoptotic effect. *Oncogene* **2009**, *28*, 781–791.
- (22) Lain, S.; Hollick, J. J.; Campbell, J.; Staples, O. D.; Higgins, M.; Aoubala, M.; McCarthy, A.; Appleyard, V.; Murray, K. E.; Baker, L.; Thompson, A.; Mathers, J.; Holland, S. J.; Stark, M. J.; Pass, G.; Woods, J.; Lane, D. P.; Westwood, N. J. Discovery, in vivo activity, and mechanism of action of a small-molecule p53 activator. *Cancer Cell* **2008**, *13*, 454–463.
- (23) Jeong, J.; Juhn, K.; Lee, H.; Kim, S. H.; Min, B. H.; Lee, K. M.; Cho, M. H.; Park, G. H.; Lee, K. H. SIRT1 promotes DNA repair activity and deacetylation of Ku70. *Exp. Mol. Med.* **2007**, *39*, 8–13.
- (24) Firestein, R.; Blander, G.; Michan, S.; Oberdoerffer, P.; Ogino, S.; Campbell, J.; Bhimavarapu, A.; Luikenuis, S.; de Cabo, R.; Fuchs, C.; Hahn, W. C.; Guarente, L. P.; Sinclair, D. A. The SIRT1 deacetylase suppresses intestinal tumorigenesis and colon cancer growth. *PLoS ONE* **2008**, *3*, e2020.
- (25) Li, X.; Zhang, S.; Blander, G.; Tse, J. G.; Krieger, M.; Guarente, L. SIRT1 deacetylates and positively regulates the nuclear receptor LXR. *Mol. Cell* **2007**, *28*, 91–106.
- (26) Mattagajasingh, I.; Kim, C. S.; Naqvi, A.; Yamamori, T.; Hoffman, T. A.; Jung, S. B.; DeRicco, J.; Kasuno, K.; Irani, K. SIRT1 promotes endothelium-dependent vascular relaxation by activating endothelial nitric oxide synthase. *Proc. Natl. Acad. Sci. U.S.A.* **2007**, *104*, 14855–14860.
- (27) Kim, D.; Nguyen, M. D.; Dobbin, M. M.; Fischer, A.; Sananbenesi, F.; Rodgers, J. T.; Delalle, I.; Baur, J. A.; Sui, G.; Armour, S. M.; Puigserver, P.; Sinclair, D. A.; Tsai, L. H. SIRT1 deacetylase protects against neurodegeneration in models for Alzheimer's disease and amyotrophic lateral sclerosis. *EMBO J.* **2007**, *26*, 3169–3179.
- (28) Gan, L.; Mucke, L. Paths of convergence: sirtuins in aging and neurodegeneration. *Neuron* **2008**, *58*, 10–14.
- (29) Lagouge, M.; Argmann, C.; Gerhart-Hines, Z.; Meziane, H.; Lerin, C.; Daussin, F.; Messadeq, N.; Milne, J.; Lambert, P.; Elliott, P.; Geny, B.; Laakso, M.; Puigserver, P.; Auwerx, J. Resveratrol improves mitochondrial function and protects against metabolic disease by activating SIRT1 and PGC-1alpha. *Cell* **2006**, *127*, 1109–1122.
- (30) Langley, E.; Pearson, M.; Faretta, M.; Bauer, U. M.; Frye, R. A.; Minucci, S.; Pelicci, P. G.; Kouzarides, T. Human SIRT2 deacetylates p53 and antagonizes PML/p53-induced cellular senescence. *EMBO J.* **2002**, *21*, 2383–2396.
- (31) Binda, O.; Nassif, C.; Branton, P. E. SIRT1 negatively regulates HDAC1-dependent transcriptional repression by the RBP1 family of proteins. *Oncogene* **2008**, *27*, 3384–3392.
- (32) Baur, J. A.; Pearson, K. J.; Price, N. L.; Jamieson, H. A.; Lerin, C.; Kalra, A.; Prabhu, V. V.; Allard, J. S.; Lopez-Lluch, G.; Lewis, K.; Pistell, P. J.; Poosala, S.; Becker, K. G.; Boss, O.; Gwinn, D.; Wang, M.; Ramaswamy, S.; Fishbein, K. W.; Spencer, R. G.; Lakatta, E. G.; Le Couteur, D.; Shaw, R. J.; Navas, P.; Puigserver, P.; Ingram, D. K.; de Cabo, R.; Sinclair, D. A. Resveratrol improves health and survival of mice on a high-calorie diet. *Nature* **2006**, *444*, 337–342.
- (33) Yang, H.; Baur, J. A.; Chen, A.; Miller, C.; Adams, J. K.; Kisielewski, A.; Howitz, K. T.; Zipkin, R. E.; Sinclair, D. A. Design and synthesis of compounds that extend yeast replicative lifespan. *Aging Cell* **2007**, *6*, 35–43.
- (34) Milne, J. C.; Lambert, P. D.; Schenk, S.; Carney, D. P.; Smith, J. J.; Gagne, D. J.; Jin, L.; Boss, O.; Perni, R. B.; Vu, C. B.; Bemis, J. E.; Xie, R.; Disch, J. S.; Ng, P. Y.; Nunes, J. J.; Lynch, A. V.; Yang, H.; Galonek, H.; Israelian, K.; Choy, W.; Iffland, A.; Lavu, S.; Medvedik, O.; Sinclair, D. A.; Olefsky, J. M.; Jirousek, M. R.; Elliott, P. J.; Westphal, C. H. Small molecule activators of SIRT1 as therapeutics for the treatment of type 2 diabetes. *Nature* **2007**, *450*, 712–716.
- (35) Nayagam, V. M.; Wang, X.; Tan, Y. C.; Poulsen, A.; Goh, K. C.; Ng, T.; Wang, H.; Song, H. Y.; Ni, B.; Entzeroth, M.; Stunkel, W. SIRT1 modulating compounds from high-throughput screening as anti-inflammatory and insulin-sensitizing agents. *J. Biomol. Screening* **2006**, *11*, 959–967.
- (36) Mai, A.; Massa, S.; Lavu, S.; Pezzi, R.; Simeoni, S.; Ragno, R.; Mariotti, F. R.; Chiani, F.; Camilloni, G.; Sinclair, D. A. Design, synthesis, and biological evaluation of sirtinol analogues as class III histone/protein deacetylase (Sirtuin) inhibitors. *J. Med. Chem.* **2005**, *48*, 7789–7795.
- (37) Bitterman, K. J.; Anderson, R. M.; Cohen, H. Y.; Latorre-Esteves, M.; Sinclair, D. A. Inhibition of silencing and accelerated aging by nicotinamide, a putative negative regulator of yeast sir2 and human SIRT1. *J. Biol. Chem.* **2002**, *277*, 45099–45107.
- (38) Sauve, A. A.; Moir, R. D.; Schramm, V. L.; Willis, I. M. Chemical activation of Sir2-dependent silencing by relief of nicotinamide inhibition. *Mol. Cell* **2005**, *17*, 595–601.
- (39) Suzuki, T.; Imai, K.; Nakagawa, H.; Miyata, N. 2-Anilinobenzenes as SIRT inhibitors. *ChemMedChem* **2006**, *1*, 1059–1062.
- (40) Cekavicius, B.; Sausins, A.; Duburs, G. Effect of substituents in the dihydropyridine ring on reactivity of the ester group of 3,5-bis-(alkoxycarbonyl)-1,4-dihydropyridines. *Khim. Geterotsikl. Soedin.* **1982**, *1072*–1077.
- (41) Hilgeroth, A.; Wiese, M.; Billich, A. Synthesis and biological evaluation of the first N-alkyl cage dimeric 4-aryl-1,4-dihydropyridines as novel nonpeptidic HIV-1 protease inhibitors. *J. Med. Chem.* **1999**, *42*, 4729–4732.
- (42) Collibee, S.; Bergnes, G.; Hamilton, M. R.; Morgan, B. P.; Morgans, D. J., Jr. Preparation of pyridine derivatives as antitumor agents to treat patient suffering from a cellular proliferative diseases. 2006-US44154, 2007059113, 20061114, **2007**.
- (43) Mai, A.; Rotili, D.; Tarantino, D.; Ornaghi, P.; Tosi, F.; Vicidomini, C.; Sbardella, G.; Nebbioso, A.; Miceli, M.; Altucci, L.; Filetici, P. Small-molecule inhibitors of histone acetyltransferase activity: identification and biological properties. *J. Med. Chem.* **2006**, *49*, 6897–6907.
- (44) Mai, A.; Rotili, D.; Tarantino, D.; Nebbioso, A.; Castellano, S.; Sbardella, G.; Tini, M.; Altucci, L. Identification of 4-hydroxyquinolines inhibitors of p300/CBP histone acetyltransferases. *Bioorg. Med. Chem. Lett.* **2009**, *19*, 1132–1135.
- (45) Marks, P. A. Discovery and development of SAHA as an anticancer agent. *Oncogene* **2007**, *26*, 1351–1356.
- (46) Sbardella, G.; Castellano, S.; Vicidomini, C.; Rotili, D.; Nebbioso, A.; Miceli, M.; Altucci, L.; Mai, A. Identification of long chain alkylidenemalonates as novel small molecule modulators of histone acetyltransferases. *Bioorg. Med. Chem. Lett.* **2008**, *18*, 2788–2792.
- (47) Ota, H.; Akishita, M.; Eto, M.; Iijima, K.; Kaneki, M.; Ouchi, Y. Sirt1 modulates premature senescence-like phenotype in human endothelial cells. *J. Mol. Cell. Cardiol.* **2007**, *43*, 571–579.
- (48) Sasaki, T.; Maier, B.; Bartke, A.; Scoble, H. Progressive loss of SIRT1 with cell cycle withdrawal. *Aging Cell* **2006**, *5*, 413–422.
- (49) Dimri, G. P.; Lee, X.; Basile, G.; Acosta, M.; Scott, G.; Roskelley, C.; Medrano, E. E.; Linskens, M.; Rubelj, I.; Pereira-Smith, O.; et al. A biomarker that identifies senescent human cells in culture and in aging skin in vivo. *Proc. Natl. Acad. Sci. U.S.A.* **1995**, *92*, 9363–9367.
- (50) Wu, Z.; Puigserver, P.; Andersson, U.; Zhang, C.; Adelmant, G.; Mootha, V.; Troy, A.; Cinti, S.; Lowell, B.; Scarpulla, R. C.; Spiegelman, B. M. Mechanisms controlling mitochondrial biogenesis



- and respiration through the thermogenic coactivator PGC-1. *Cell* **1999**, *98*, 115–124.
- (51) Nebbioso, A.; Clarke, N.; Voltz, E.; Germain, E.; Ambrosino, C.; Bontempo, P.; Alvarez, R.; Schiavone, E. M.; Ferrara, F.; Bresciani, F.; Weisz, A.; de Lera, A. R.; Gronemeyer, H.; Altucci, L. Tumor-selective action of HDAC inhibitors involves TRAIL induction in acute myeloid leukemia cells. *Nat. Med.* **2005**, *11*, 77–84.
- (52) Altucci, L.; Rossin, A.; Raffelsberger, W.; Reitmair, A.; Chomienne, C.; Gronemeyer, H. Retinoic acid-induced apoptosis in leukemia cells is mediated by paracrine action of tumor-selective death ligand TRAIL. *Nat. Med.* **2001**, *7*, 680–686.
- (53) Campisi, J. Cancer, aging and cellular senescence. *In Vivo* **2000**, *14*, 183–188.